Adaptive optics for wide-field microscopy

Bourgenot, C., Saunter, C., Girkin, J., Love, G.

C. Bourgenot, C. D. Saunter, J. M. Girkin, G. D. Love, "Adaptive optics for wide-field microscopy," Proc. SPIE 7904, Three-Dimensional and Multidimensional Microscopy: Image Acquisition and Processing XVIII, 790414 (23 February 2011); doi: 10.1117/12.873857

SPIE.

Event: SPIE BiOS, 2011, San Francisco, California, United States

Adaptive Optics for Wide-field Microscopy

C. Bourgenot, C.D. Saunter, J.M. Girkin, G.D. Love
Centre for Advanced Instrumentation, Department of Physics, Durham University, South Road, Durham, DH1 3LE, UK

ABSTRACT

We report on recent developments in the use of adaptive optics (AO) in wide-field microscopy to remove both system and sample induced aberrations. We describe progress on using both a full AO system and image optimization techniques (wavefront sensorless AO). In the latter system the determination of the best mirror shape is found via two routes. In the first an optimization algorithm using a Simplex search pattern is used with an initial random set of mirror shapes. We then explore the use of specific Zernike terms as our starting basis set. In both cases the final optimization performance is not affected by the choice of optimization metric. We then describe an open loop AO system in which the equivalent of a laser guide star is used as the light source for the wavefront sensor.

Keywords: Optical Microscopy, Aberration correction, Adaptive Optics

1. Introduction

Optical microscopy is still the main research tool for many biological studies. Indeed with the advent of genetic manipulation and specifically the use of fluorescent protein expressing in animals and plants it has actually seen a renaissance in the past ten years, in particular with the development of novel techniques such as CARS, PALM, STORM, STED and SPIM. Previously much optical microscopy was undertaken on fixed and ultra-thinly sliced samples, however what the life scientist really requires is the ability to see intact and living tissue. In all of these methods described above, as well as now more conventional confocal, multiphoton and structured illumination methods, one has to look through the sample at some point. The sample thus adds an additional and uncontrolled optical path to the sample, which leads to aberrations in the final image.

Significant work has been undertaken in attempting to explore these aberrations and it is beyond the scope of this paper to describe in detail the literature [1] but they come about in general due to refractive index mismatches within the sample. The aberrations thus caused are high order (not simply defocus, astigmatism etc) and do not lend themselves to compensation through a single optical element, though to some extent spherical aberration can be removed either using a multi-immersion lens and adjusting the correction collar, or through the addition of a lens in the optical path. In addition to the sample aberrations there are typically some system aberrations present even in the best designed system of mirrors and lenses, particularly in complex beam scanning systems. Thus to obtain the best possible images the user would like to remove these unwanted aberrations which can cause image degradation and even potentially artifacts within the image.

AO was originally developed for use in ground based astronomical telescopes to remove atmospheric turbulence [2]. Here the optical aberration is generally determined through the use of a guide star (either real or generated using a laser) and a wavefront sensor and the inverse aberration placed on the deformable mirror to compensate for the original aberration. High performance AO on ground based telescopes can now frequently produce better quality images than space-based telescopes (since ground based telescopes typically have larger apertures). Astronomical AO continues to be extremely expensive, but through the development of MEMS and liquid crystal based technology it is now possible to construct lower cost AO systems. The move into optical microscopy has taken place on the back of these commercial developments.

The original work on AO in microscopy was undertaken on beam scanning systems [3,4,5] demonstrating what can be gained through the use of such technology and this was then implemented in a wide field microscope to overcome the

Three-Dimensional and Multidimensional Microscopy: Image Acquisition and Processing XVIII,
edited by Jose-Angel Conchello, Carol J. Cogswell, Tony Wilson, Thomas G. Brown, Proc. of SPIE Vol. 7904
790414 · © 2011 SPIE · CCC code: 1605-7422/11/$18 · doi: 10.1117/12.873857

system aberrations when zooming in through a lower numerical aperture lens [6]. All of these systems used an optimization algorithm in some form to determine the aberration correction required, and this continues to be the general situation though this has recently come to be termed "wavefront sensorless" correction. The selection of the correct optimization algorithm has been explored before [7] but here we concentrate on the detailed performance of different metrics considering which may be the most suitable, before discussing an open loop AO system

2. Method

2.1. Optimization System Description

The optical system concept is shown in figure 1.

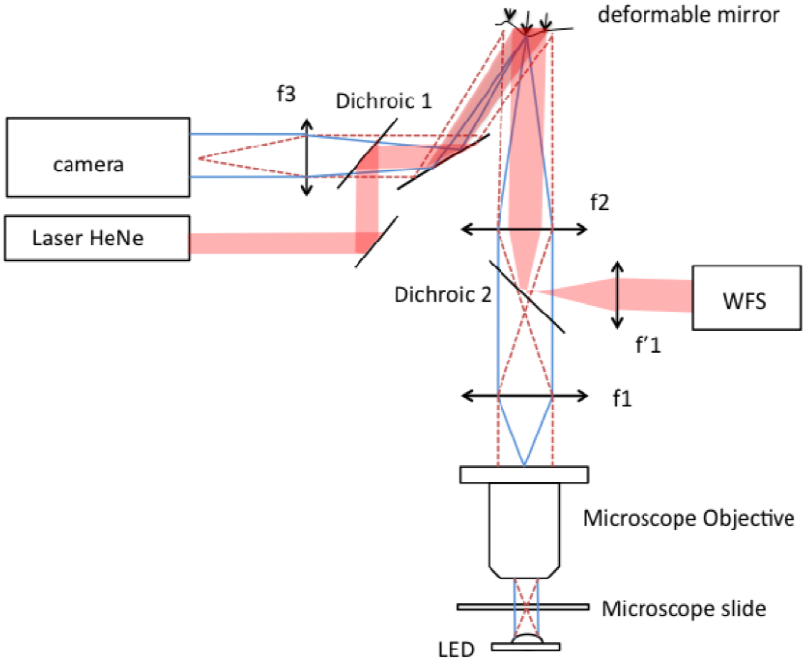

Figure 1. Overall system configuration for optimization AO in a wide field microscope.

Light from an LED is used to illuminate the sample which can either be operating in fluorescent or transmission mode. We presently do not use an epi-illumination configuration as our work is aimed toward the use of AO in selective plane illumination microscopy [8]. The light then passes through the collection objective (typically Nikon S-Plan Fluor 40x 0.6) and is imaged onto a camera (Q-imaging Inc) via the deformable mirror. Dichroic beamsplitters are used to ensure that only the sample light reaches the detector thus blocking the laser or excitation source. The laser is directed toward the sample, via the deformable mirror and on to a Shack-Hartmann wavefront sensor (Thor Labs Inc). The control software was custom written, as opposed to the commercially supplied software. This beam is solely used to determine the shape of the deformable mirror and in this system, plays no part in the determination of the shape to be placed onto the mirror.

In the work to date we have used a wide variety of mirrors and all are found to work in the system. These mirrors include devices supplied by Boston Micro Machines, Imagine Optic, OkoTech, and Adaptica and are generally those with a low number (around 40) of actuators. In the case of mirrors, which can only be pulled from their neutral position, we bias the

mirror so that it is initially in the mid-point of its travel. The control of the mirror is achieved via the commercially supplied electronics which all interface to the control computer via a USB link.

2.2. Optimization Software

Full details of the software routines is being prepared for a full journal publication but an outline is provided here. All routines are written in Python and interfaced with C++ calls when required by the commercial drivers to control the mirror shape. A graphical interface has been built which enables the camera image to be displayed and a region of interest selected for the optimization algorithm to analyze. Options are provided on the metric to be used and the metric value is displayed in a real time graph. The mirror shape is also displayed with false color to express the wavefront distortion as a set of Zernike terms. The system is capable of recording all of the images and wavefronts produced for later analysis.

In the present system we have incorporated metrics which include, Fast Fourier Transform mask, Intensity squared, Sobel Filter, Image variance and Wavelet based analysis. All have been implemented in Python and follow standard patterns for image analysis software and are thus not described in detail here. The performance of these metrics was initially evaluated on non-microscope images to ensure that they were operating correctly. The actually optimization is undertaken using a Simplex algorithm which has previously been used by our group for astronomical applications and thus its behavior is well characterized. In brief for a mirror with N actuators we require $N + 1$ initial mirror shapes and these are generated through a look up table after a series of experiments to determine the best basis set to start.

In the Zernike guided optimization the $N + 1$ mirror shapes consist of six Zernike terms (spherical, astigmatism at two angles and coma at two angles) with different randomly chosen levels being applied to fill the full starting basis set for the Simplex routine. Exact level of Zernike term can also be applied, but it requires an initial estimation of each individual aberration amplitude.

2.3. Open Loop Optical Configuration

The optical system for the open loop system is shown in figure 2 .

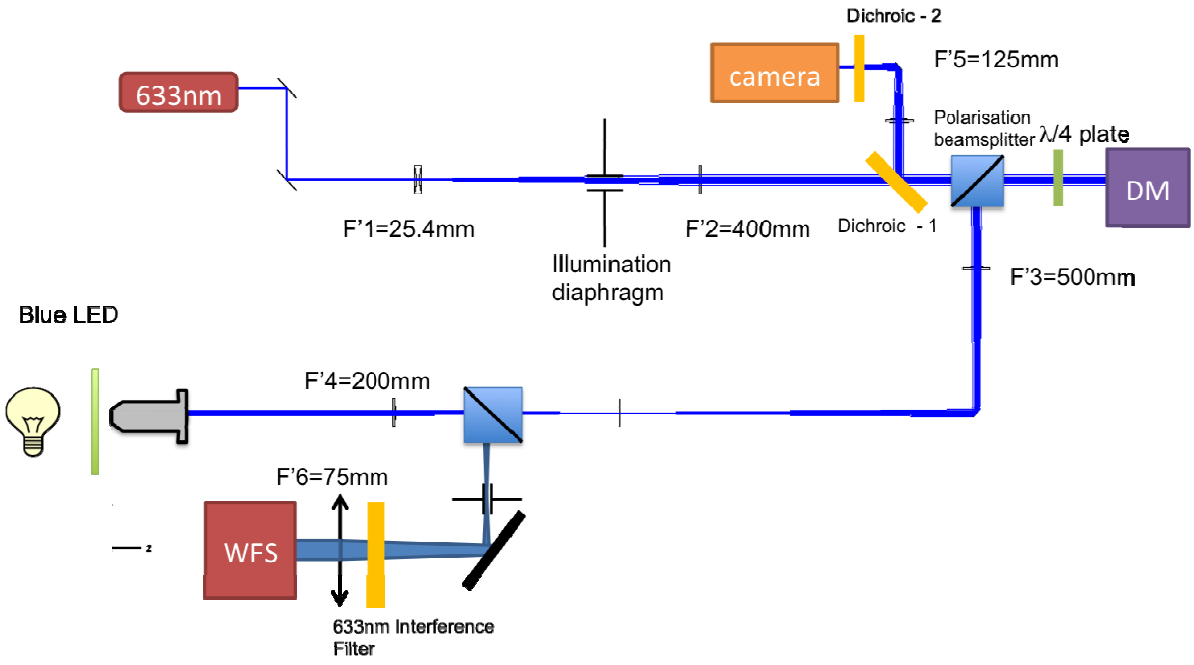

Figure 2. Open loop AO optical imaging system

The sample illumination is identical to that described in the previous system with the image from the objective being imaged onto the deformable mirror via a polarizing beamsplitter cube and quarter waveplate before passing onto the science camera (Q-Imaging Inc) via a dichroic mirror. The focal length of the lenses was selected for convenience in making the system small enough to fit onto an optical breadboard and also for producing an image on the camera with sufficient magnification. The beam on the wavefront sensor path has also been largely reduced to allow an optimized sampling by the microlens of the wavefront sensor in view to optimize the speed of the system.

In this system the helium neon laser forms the equivalent of a laser guide star in an astronomical system within the sample. The light at 633 nm is initially expanded to fill the deformable mirror with a pin hole acting as a spatial filter included in the system to ensure a good beam quality on the sample. The deformable mirror is then imaged onto the back aperture of the objective lens using beam expansion when required. The exact value of the lenses is determined by the size of the deformable mirror being used. The dimension in the system above are for a mirror with an aperture of around 15 mm, filling about 12 mm of the mirror. The laser light reflected back from the sample is then directed onto a wavefront sensor which is again conjugated with the back pupil plane of the objective. A laser line filter is used to ensure that only reflected laser light reaches this detector.

In operation the distortion of the reflected laser spot is determined by the control computer which then sends the appropriate shape to the mirror as a series of Zernike terms which have previously been determined for the mirror so that the mirror produces wavefront modes which are as close as possible to a pure series of low order Zernike modes as possible - with the exception of tip, tilt and defocus which could alter the image plane of the system. In addition an adjustable pinhole is used before the sensor to make the system so as to select the laser light from a particular depth plane. The is therefore"slightly confocal" but care was taken to ensure that the laser mode was not spatially filtered before the wavefront sensor. This system forms an open loop, which is constantly trying to produce a "perfect" shape on the deformable mirror. The science camera is continually streaming images to the computer whilst the open loop controls the mirror shape. The update rate of the loop is around 10 Hz. System aberrations can be added using distorted glass. This enables the system to be optimized using a constant aberration before a wide range of aberrations are added through the biological samples.

3. Results

Full details of the performance of the system are in to be submitted shortly but the highlights of the results are presented below. Figure 3 shows the performance of the five optimization metrics used undertaking an optimization on the sample (murine dorsal tissue incorporating with GFP expressing skin stem cells, sample courtesy of Dr Carrie Ambler and Dr Richie Wong, Durham University)

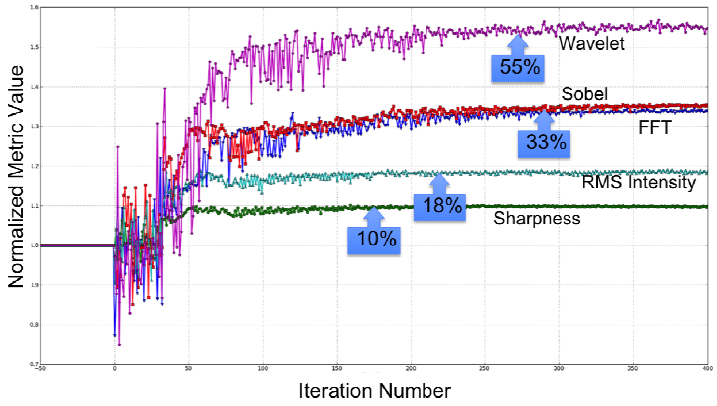

Figure 3. Metric Optimization Performance. The metric value is shown as a function of iteration number for various image metrics.

It can clearly be seen from the figure that all optimization metrics converged and in similar timescales (iteration numbers). The percentage improvement in each metric is shown and these would appear to indicate that the wavelet metric performed best but this is misleading. Although the different algorithms produced different percentage improvements the overall improvement in image quality was similar in all cases. This was tested by comparing the final images optimized with different metrics with the single metric. In all cases no matter which original metric was used the final metric value was the same for each metric method. These tests were repeated several times on different samples and the same result was found each time. We believe that we can thus state, at least for this system, that the final result is weakly dependent of the metric selected. Further work was also undertaken looking at the effect of different Zernike terms of the various metric values and all plots of metric value against Zernike distortion showed the same shape (Figure 5), further indicating that the metrics all perform in a similar manner for the samples imaged.

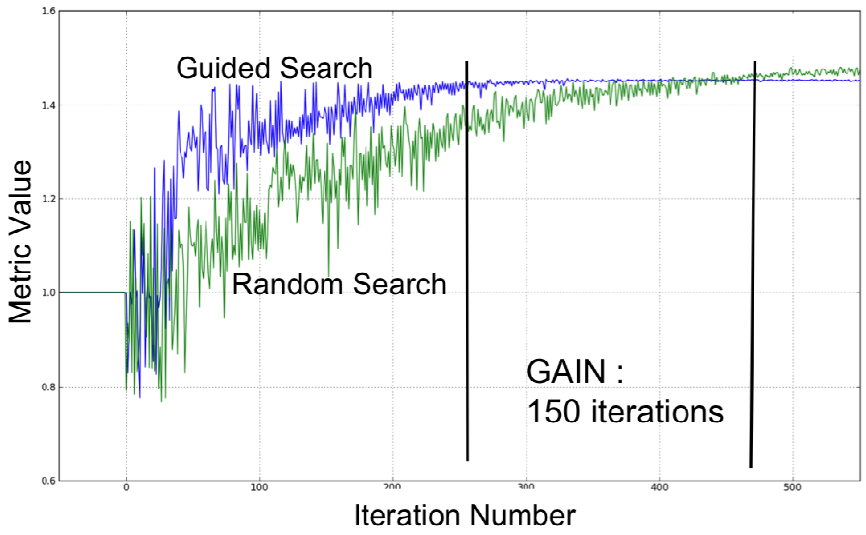

Figure 4. Metric value verses iteration number for a search guided by Zernike terms using a Sobel metric versus a random search.

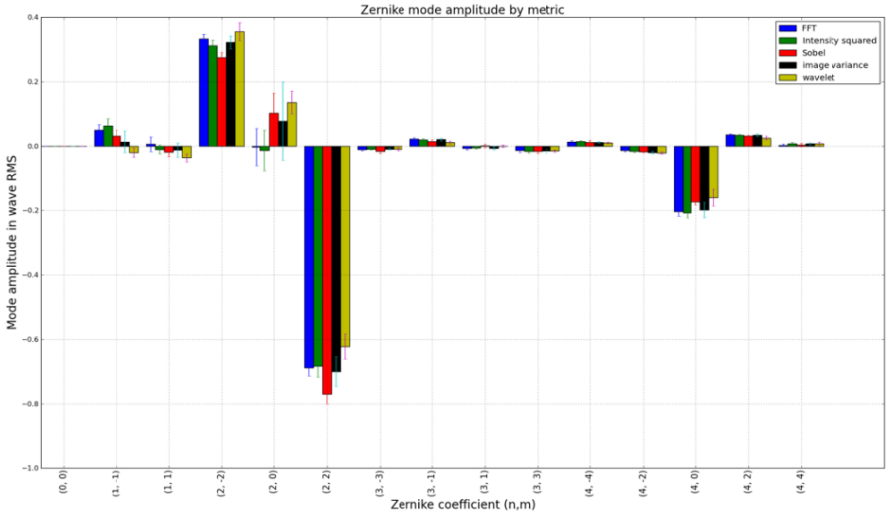

Figure 5. Deformable mirror Zernike amplitude mode by metric after optimization for different search metrics – showing the results are essentially independent of search metric.

The figure 4 clearly illustrates the decrease in the number of iterations used when specific Zernike terms were used in the Simplex optimization algorithm. The example shown uses a Sobel metric but all of the metrics discussed above showed a similar trend. Crucial to this improvement is the fact that "tip" and "tilt" were specifically excluded from the Zernike set. This meant that there was a significantly reduced risk of the selected region of interest being used for the optimization metric did not move outside the selected region of interest. It was seen in all cases that in the initial stages of the optimization that the variation (or noise) in the metric value was reduced and this is also visible in figure 4 at around 100 iterations in the random search (lower) curve.

The open loop system was also run on a range of samples, frequently to date non-biological systems in order to make quantified measurements in the system in real time. These are best displayed as videos and thus not suitable for print publication but a pollen grain image is shown below to illustrate the improvement in the image quality. The images are raw images as captured by the camera.

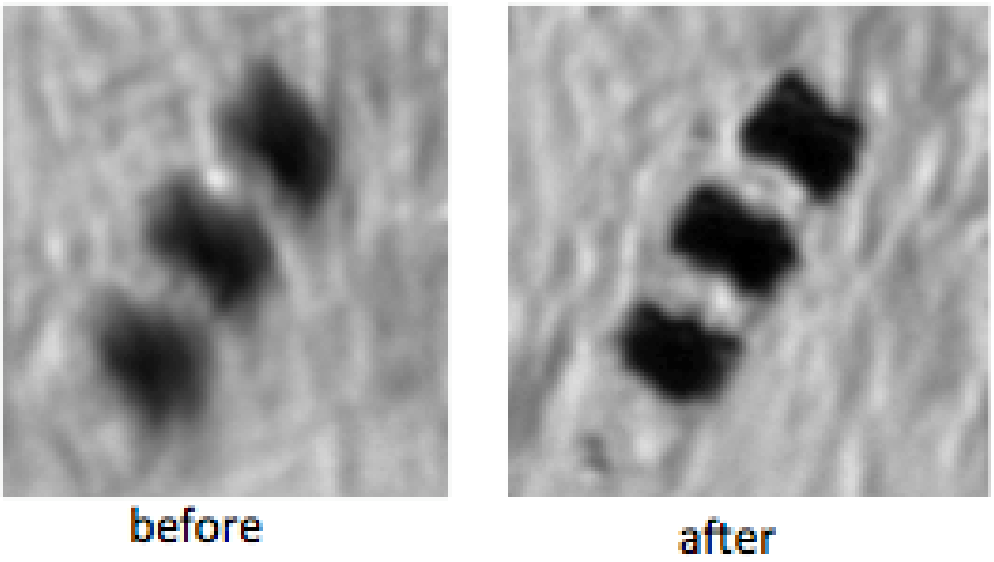

Figure 5. Raw images of mouse back skin tissue before and after open loop adaptive optics, field of view 23 microns

4. Conclusions and Discussions

We have demonstrated that adaptive optics can be implemented in a wide field microscope using both optimization algorithms and open loop control using a wavefront sensor to determine the correct deformation to be applied to an adaptive optics mirror to remove both system and sample induced aberrations. There is strong evidence to indicate that the selection of the metric in optimization based methods is not crucial, but that the use of specific aberrations (Zernike terms) improves the speed of optimization. We have also demonstrated that wide field open loop AO control is possible using light from a laser as the equivalent of a laser guidestar. We now aim to extend the techniques to closed loop operation and will consider other wide field techniques [9].

Acknowledgements

The authors wish to acknowledge funding from the British Heart Foundation, in particular a Research Excellence Award, the Engineering and Physical Science Research Council. All samples were used in accordance with UK Home Office rules

References

1. Girkin J.M., Poland S., and Wright A.J "Adaptive optics for deeper imaging of biological samples", Current Opinion in Biotechnology, **20,** 106-110, (2009)
2. Tyson R. K., "Principles of Adaptive Optics", Academic Press, (1997)
3. Sherman L., Ye J. Y., Albert O., Norris T. B., "Adaptive correction of depth-induced aberrations in multiphoton scanning microscopy using a deformable Mirror", Journal of Microscopy, **206**, 65-71 (2002)
4. Booth M.J., Neil M.A.A., Juskaitis R., Wilson T. "Adaptive aberration correction in a confocal microscope", Proceedings of the National Academy of Sciences, **99**,5788-5792 (2002)
5. Marsh P.N., Burns D., Girkin J.M.**, "**Practical implementation of adaptive optics in multiphoton microscopy", Optics Express, **11**, 1123-1130 (2003)
6. Potsaid B., Bellouard Y., Wen J.T., "Adaptive Scanning Optical Microscope (ASOM): A multidisciplinary optical Microscope design for large field of view and high resolution imaging", Optics Express **13**, 6504-6518 (2005)
7. Poland S.P., Wright A.J., Girkin J.M., "Evaluation of fitness parameters used in an iterative approach to aberration correction in optical sectioning microscopy", Applied Optics, **47**, 731-736 (2008)
8. Huisken J., Swoger J., Del Bene, F., Wittbrodt J., Stelzer E.H.K., "Optical sectioning deep inside live embryos by selective plane illumination microscopy", Science, **305**, 1007, (2004)
9. Langlois, M., Saunter, C.D., Dunlop, C.N., Myers, R.M., and Love, G.D. "Multiconjugate adaptive optics: laboratory experience," *Opt. Express,* **12,** 1689-1699 (2004).